Mixed Convection Transport from a Protruding Heat Source Module on a Vertical Surface

B. H. Kang* and Y. Jaluria†
Rutgers, The State University of New Jersey, New Brunswick, NJ 08903

An experimental study of mixed convective transport from a protruding heat source module mounted on a vertical surface in an externally induced flow has been carried out. This problem is of particular interest in the design of thermal systems, such as the cooling of electronic circuitry and positioning of a heating element in a furnace. The temperature and velocity distributions are measured. The dependence of the heat transfer rate and of the thermal field on the mixed convection parameter and on the thickness of the heat source module, particularly in the vicinity of the source, are investigated in detail. Experimental results indicate that the flowfield and the temperature distribution in the flow over the module are substantially affected by the module thickness and also by the mixed convection parameter due to the combined effects of the forced convection flow and of the buoyancy-driven flow arising from the heat input. These, in turn, have a strong influence on the convective heat transfer from the heat source to the ambient. The thermal and viscous boundary layers as well as the variation of the surface temperature are determined and the results discussed in terms of underlying physical processes. The results obtained are also compared with those for an element of negligible thickness. Thus, the effect of a significant module thickness on the convective transport is determined.

Nomenclature

A = total surface area of the module exposed to the fluid
g = gravitational acceleration
Gr = Grashof number, defined in Eq. (2)
h = local, convective, heat transfer coefficient
$\bar{h}$ = average, convective, heat transfer coefficient
H = thickness of the heated module
k = thermal conductivity of the fluid
L = height of the heated module, shown in Fig. 1
L_1 = distance from the leading edge of the plate to the heat source module
$\underline{Nu}$ = local Nusselt number, hL/k
$\overline{Nu}$ = mean Nusselt number
q = uniform heat flux input at the module surface due to the electrical power dissipation
q_{cond} = heat flux conducted from the heat source to the test plate
q_{conv} = heat flux convected from the heat source to the flow
Q = total heat input, per unit width, into the module, $Q = q(L + 2H)$
Re = Reynolds number, defined in Eq. (2)
s = distance along the module, shown in Fig. 8
T = local temperature
T_a = ambient temperature
T_s = local surface temperature
U = local velocity in x direction
U_0 = forced flow velocity
U_{max} = local maximum flow velocity
W = width of the heated module
x = distance along the vertical surface measured from the bottom of the module, shown in Fig. 1
X = dimensionless x coordinate, defined in Eq. (1)
y = horizontal coordinate distance from the plate surface, shown in Fig. 1
Y = dimensionless y coordinate, defined in Eq. (1)
β = coefficient of thermal expansion of the fluid
ν = kinematic viscosity of the fluid
θ = dimensionless local temperature, defined in Eq. (1)
θ_s = dimensionless surface temperature

Received July 28, 1989; revision received Nov. 6, 1989.

*Graduate Research Assistant, Department of Mechanical and Aerospace Engineering.
†Professor, Department of Mechanical and Aerospace Engineering.

Introduction

A PROBLEM of considerable practical and fundamental interest is that of the mixed convective heat transfer from an isolated heat source located on a surface. Energy dissipating devices and panels act as thermal sources and generate a natural convection flow. In many cases, a forced flow is employed for increasing the thermal transport from such an isolated heat source. The effect of the incorporation of both natural and forced convection mechanisms on the heat transfer rate is particularly important in the design and operation of thermal systems, such as in the cooling of electronic circuitry and the positioning of heating elements in furnaces.[1-4] Of particular interest is the effect of the wake generated by a heated rectangular module on the flow and thermal field near the module since the heat transfer is determined by the temperature of the adjacent fluid. Therefore, it is important to investigate the velocity and thermal fields and also their dependence on the physical parameters, such as the external velocity, energy input, and thickness of the heat source module in such problems.

Considerable work has been done on the heat transfer from an isolated heat source on surface. The natural convection flows generated by isolated line, point, and finite-sized thermal sources have been studied. The boundary-layer flow due to a line thermal source on an adiabatic vertical surface may be solved using the similarity method.[5] This approach cannot be applied for studying the flow over a finite-sized thermal source. Then, the laminar boundary-layer equations may be solved by finite-difference methods.[6] Some experimental work has also been done by several investigators.[7,8] In all these investigations, the heat source was mounted flush on the surface. Recently, experimental and numerical studies have been carried out on the natural convective cooling of a protruding heat source module mounted on a vertical wall.[9,10]

In response to the cooling needs of certain applications, a forced flow may be employed to enhance the heat transfer, for instance, in high-power dissipating systems. Considerable at-

tention has been directed at forced and mixed convection heat transfer from an isolated heat source. A thermal analysis has been carried out on the forced air cooling of a protruding heat source in a constricted channel using finite-difference methods.[11] Forced convective cooling of multiple rectangular blocks with uniformly distributed heat flux has also been studied.[12] Some work has been directed at the corresponding mixed convection flow resulting from the addition of a specified flow velocity to a natural convection flow. Kennedy and Zebib[13] presented numerical and experimental results on the buoyancy effects in a laminar horizontal channel flow with an isolated heat source on the lower or upper wall. They found that the natural convection effects led to a recirculating region adjacent to the top wall, above the heat source. The effect of an externally induced forced flow on the heat transfer rate from a single heat source has been investigated theoretically.[14,15] However, very little work has been done on mixed convective flow over a heat source module with significant thickness. An experimental study of mixed convective transport from such a heat source placed on a horizontal surface has been carried out earlier.[16]

The present study is directed at the mixed convection transport from an isolated, protruding heat source module mounted on a vertical, well-insulated surface through a detailed experimental investigation. The physical model and the coordinate system considered are shown in Fig. 1. The vertical surface and the heat source module are taken wide enough in the transverse direction so that a two-dimensional flow situation is obtained. The temperature distribution in the flow and at the surface as well as the velocity distribution are measured. The effects of the externally induced flow velocity, heat input, and the thickness of the heat source module on the heat transfer rate and on the thermal field, particularly in the vicinity of the source, are studied in detail.

Experimental Arrangement

The experimental setup consists of a vertical, low-speed wind tunnel with a test section 61 × 46 cm in cross-sectional area and 150 cm in length. These dimensions ensure that an experimental setup placed inside the test section is far from the walls and is, thus, free of the wall effects. A schematic diagram of the experimental arrangement is shown in Fig. 2. A uniform flow, with velocity ranging from 0 to 50 cm/s, is obtained in the test section by means of a blower, whose flow rate can be varied. The flow from the blower enters the test section through a honeycomb section and a fine-mesh screen. This arrangement provides a fairly uniform flow with negligible turbulence with intensities less than 5% in the test section. The uniformity of the flow and the turbulence level were checked by extensive hot wire anemometry measurements. The heat source module consists of a highly polished, stainless steel foil (0.03 mm thick) wrapped around a stack of several bakelite strips (2.2 cm long, 1.5 mm thick, and 40 cm wide). A thermally-conducting epoxy cement was employed to ensure good contact. The thickness of the module can be varied by changing the number of strips in the stack. The stainless steel foil is electrically heated to provide a uniform heat flux input condition over the module surface.

The heat source module is mounted firmly on a vertical plate by means of a specially designed clamp, and the entire assembly is placed in the test section of the wind tunnel. In order to reduce the conduction heat losses from the heat source to the plate, the plate is made of three parallel thin masonite boards separated by 6-mm air gaps. With this arrangement, the conduction through the air gaps was estimated to be less than 10% of the total electrical heat input.[17] Radiative losses are also kept low by employing a polished stainless steel foil. The emissivity of stainless steel foil was experimentally found to be of the order of 0.1.[7] The radiation heat loss to the ambient was calculated to be less than 3% of the total electrical power dissipation for the heat flux range considered.[16] The discussion on the convective heat flux measurement is given later.

The electric power dissipation in the foil is obtained by measuring the voltage drop across the strip and the current through it by means of a precision digital voltmeter and an ammeter, respectively. Three high temperature heat flux gauges (RdF Corp., Model 270310-20) are mounted evenly at the backside of each heating foil to measure the conductive heat flux from the foil to the test plate. In addition to these gauges, six more high sensitivity heat flux gauges are mounted on the vertical plate at downstream locations of the module in order to obtain the local convective heat flux from the plate. The heat flux gauge consists of a heat flow sensor and a thermocouple. The thickness, conductivity, and response time of the heat flow sensor are 0.5 mm, 0.112 $W/(m°C)$, and 0.4 s, respectively. Thus, the resulting thermal resistance of the heat flow sensor is 0.0447°C m^2/W. Here, thermal resistance is the temperature difference between the front surface and rear-mounting surface of the sensor per unit of heat flow through the sensor. The thermocouple to the heat flux gauge measures the surface temperature at the exact location where the heat flux is measured. The heat flux data are recorded by means of a data acquisition system (Keithley, Series 500).

The surface temperature is measured using a set of 30 thermocouples (Copper-Constantan, 0.025-mm-diam wire) attached to the module and vertical surface by means of a high thermal conductivity cement. The temperature and velocity in

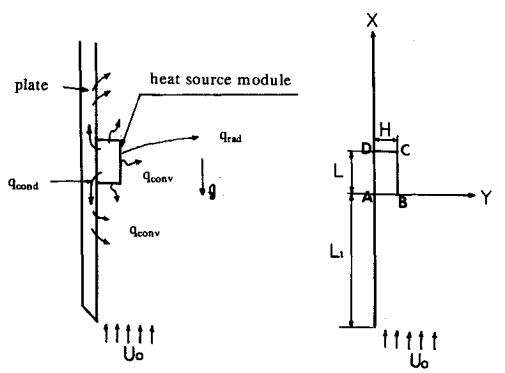

a) Physical model b) Coordinate system

Fig. 1 Physical model and the coordinate system.

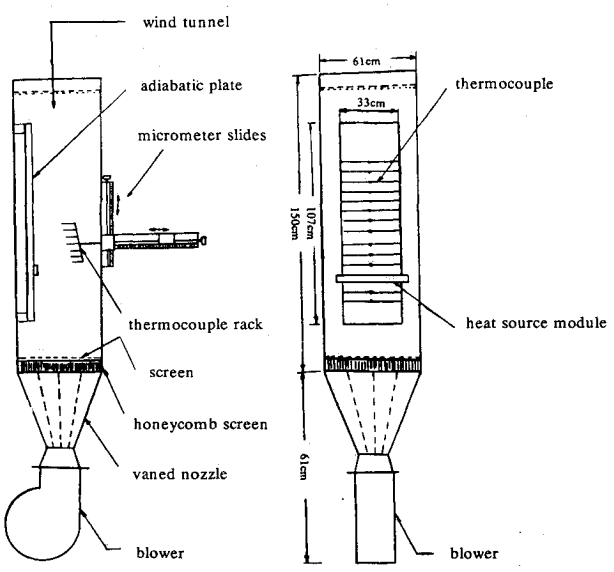

a) Side view b) Front view

Fig. 2 Experimental arrangement.

the flow are measured by a set of seven thermocouples (Copper-Constantan, 0.05-mm diam wire) and by a constant temperature hot wire anemometer (DISA), respectively. Thermocouples are staggered in the direction of the flow in order to avoid interference between each other. A probe assembly is used with a traversing arrangement to position the thermocouple and hot wire at any desired location in the flow. A hot-wire calibration system for the low velocity levels encountered here has been developed, and calibration charts were obtained over a velocity range from 0 to 50 cm/s. The calibration for variable fluid temperature was obtained by varying the overheat ratio.[18] A data acquisition system, which employs an analog-to-digital converter with an Apple microcomputer, is used for storing the data for subsequent analysis and graphics on a Sun computer system. The error was estimated to be within about $\pm$ 1% for the temperature measurements, about $\pm$ 3% for the velocity measurements, and about $\pm$ 3% for the heat flux measurements of the measured value. These errors correspond to about 0.5°C in the measured temperature, about 3 mm/s in the velocity, and 30 W/m^2 in the heat flux. Repeatability to within $\pm$ 5% was obtained in all the measurements, including that for the heat transfer coefficient, lending strong support to the accuracy of the results obtained and to the consistency of the experimental scheme. The error analysis of measurements, based on the relative uncertainty, is discussed in detail later.

A fairly wide range of the governing parameters, particularly the mixed convection parameter and the module thickness, was considered. However, the ranges employed correspond largely to flows of interest in the electronic packaging industry and manufacturing systems. Moreover, interest was mainly directed at circumstances where the buoyancy effects are significant. The pure natural or the pure forced convection cases were not studied in detail since the mixed convection flow was of particular interest in this study.

Experimental Results and Discussion

The basic physical parameters in the problem under consideration are the heat flux input q, the height L and the thickness H of the heat-source module, the distance L_1 from the leading edge of the plate to the heat-source module, and the forced flow velocity U_0 (see Fig. 1). As mentioned earlier, the freestream turbulence was negligible in this study. The relevant dimensionless quantities may be derived from these physical variables taking the height L of the module, which is kept constant as 2.2 cm, as the characteristic dimension. The distance of the module from the leading edge of the plate L_1 is taken at a fixed value of $L_1/L = 8$ here, for convenience, in the presentation of the results. In fact, L_1/L is an important parameter in the flow if the heat source module is placed near the leading edge of the plate. However, the basic trends are observed to remain unchanged with varying values of L_1/L over the range 6–10. The coordinate system employed is shown in Fig. 1.

The results obtained are presented in terms of the dimensionless temperature θ and the dimensionless coordinate distance X and Y for a uniform heat flux q at the heated region, defined as

$$\theta = \frac{(T - T_a)}{(L + 2H)/k} Gr^{1/5}, \quad X = \frac{x}{L}, \quad Y = \frac{y}{L} \tag{1}$$

where

$$Gr = \frac{g\beta q\,(L + 2H)L^3}{kv^2}, \qquad Re = U_0 \frac{L}{v} \tag{2}$$

These are the dimensionless variables frequently employed for the uniform heat flux circumstance.[14,19] The heat input into the heated element per unit width Q is given by $q\,(L + 2H)$. Therefore, the characteristic temperature difference in this formulation becomes $[q(L + 2H)/k]$ instead of $T_s - T_a$, where T_s is the surface temperature for the isothermal case. Properties of the fluid are evaluated at the local film temperature $(T_s + T_a)/2$. The definition of the Grashof number and the dimensionless temperature θ may be based on an average convected heat flux since local convective heat fluxes are determined in this study. However, the actual measured quantity is the total energy input, which is therefore appropriate for the definition of Gr. Also, both the conduction and the radiation heat losses are kept low, estimated to be 10–13% of the total heat input. Thus, the total convective transport from the module is generally around 90% of the total energy input. However, the ratio of the local convective heat flux to the total heat flux input varies with location and can be as low as 0.75–0.93. (See Ref. 16 for more detailed discussion on this aspect.) The resulting trends obtained here are not expected to be significantly affected if the total convective heat transfer rate is employed for nondimensionalization instead of Q.

The effect of the forced flow on the thermal field in the flow is shown in Figs. 3a–3c. In this figure, isotherms are shown for a fixed Grashof number $Gr = 2.3 \times 10^6$ and three values of the Reynolds number $Re = 435$, 350, and 295. The temperature level increases over the module due to the heat input and then decreases gradually downstream from the module, as expected, for all cases of Re. The isotherms move toward the surface downstream whereas these were found to move away from the surface downstream of the module when the module is placed on a horizontal surface.[16] The observation can be attributed to the fact that the thermal buoyancy force is aligned with the forced flow on the vertical surface considered here whereas the buoyancy force is normal to the forced flow

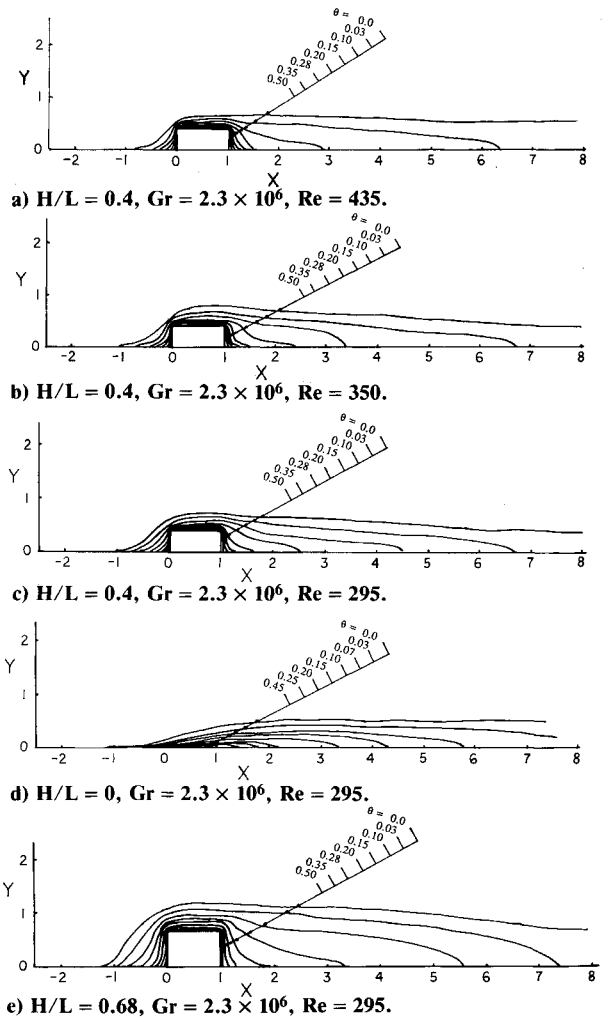

a) H/L = 0.4, Gr = 2.3 × 10⁶, Re = 435.

b) H/L = 0.4, Gr = 2.3 × 10⁶, Re = 350.

c) H/L = 0.4, Gr = 2.3 × 10⁶, Re = 295.

d) H/L = 0, Gr = 2.3 × 10⁶, Re = 295.

e) H/L = 0.68, Gr = 2.3 × 10⁶, Re = 295.

Fig. 3 Measured thermal field, shown as distribution of isotherms in the flow.

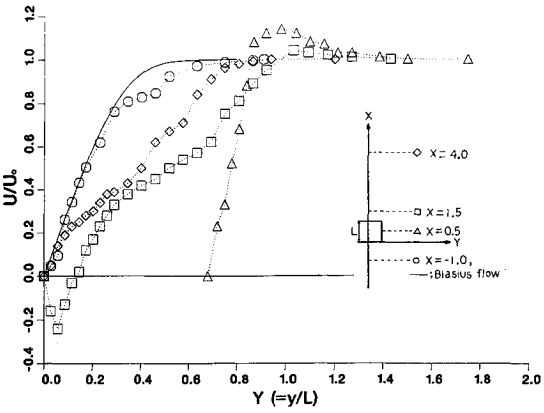

Fig. 4 Measured velocity profiles at various downstream locations for $H/L = 0.68$, $Gr = 2.3 \times 10^6$, and $Re = 295$.

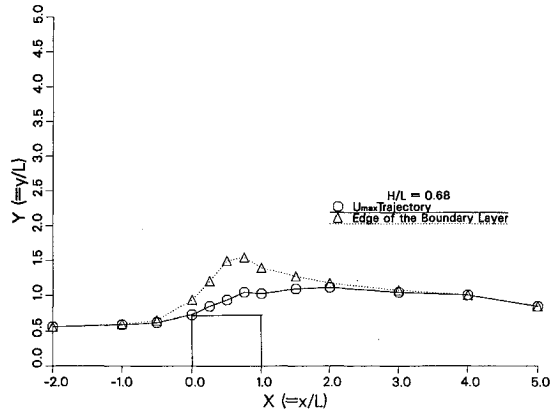

Fig. 5b Variation of the local maximum velocity along the plate for $Re = 295$, $Gr = 2.3 \times 10^6$, and $H/L = 0.68$.

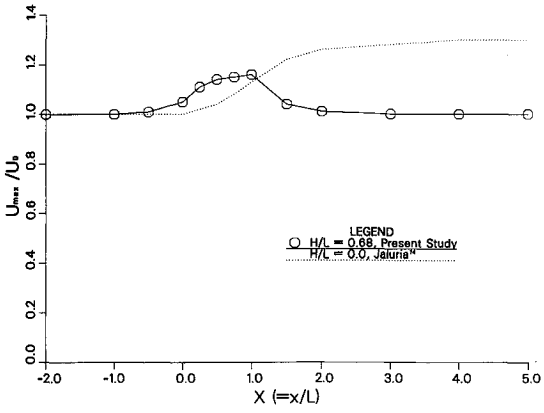

Fig. 5a Location of the edge of the viscous boundary layer and the trajectory of the local maximum velocity in the flow for $Re = 295$, $Gr = 2.3 \times 10^6$, and $H/L = 0.68$.

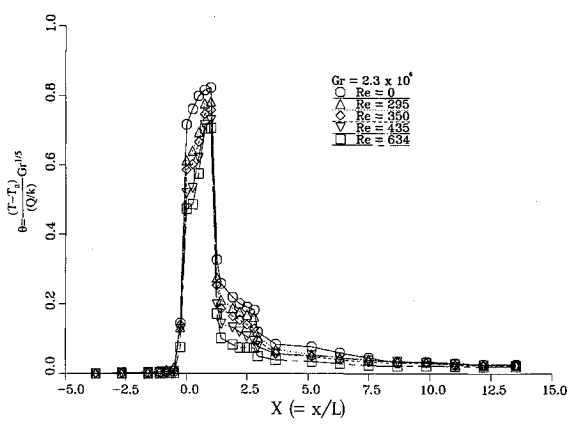

Fig. 6 Surface temperature distribution for $H/L = 0.4$ at $Gr = 2.3 \times 10^6$ for different values of Re.

direction for the horizontal case. This leads to the flow moved away form the surface resulting in separation if the buoyancy effects are strong enough.[19] However, the trends in the vertical case are similar to those for forced convection flow, i.e, negligible buoyancy effects, in the horizontal case. The effect of the module thickness on the thermal field is shown in Figs. 3c and 3e at $Re = 295$ and $Gr = 2.3 \times 10^6$. It is seen that the thicker module has a stronger influence on the distortion of the forced flow and on the resulting temperature distribution in the flow over the module.

Figure 4 shows the downstream variation of the measured velocity profiles with the dimensionless distance Y from the surface at various X locations. The results are shown for $H/L = 0.68$, $Gr = 2.3 \times 10^6$, and $Re = 295$. The velocity profile at $X = -1$ is compared with that for forced convection flow over a module with negligible thickness. As seen in this figure, the measured values are lower than the predicted results for the forced convection flow. This is a consequence of the effect of both the module thickness and the natural convection effect at the bottom surface (A-B, in Fig. 1) of the module. At the midpoint of the module, $X = 0.5$, the velocity increases sharply near the module due to the strong effect of the buoyancy force to reach a maximum. It then decreases gradually to the forced flow velocity. Reverse flow is observed at downstream locations near the top surface of the module. The magnitude of the reverse flow is found to be small compared to the forced flow velocity because of the viscous effect of the vertical wall. At a location far downstream, $X = 4$, neither the reverse flow nor the peak in the velocity profile is observed. This result implies that the downstream location at $X = 4$ is far from the reattachment area of the flow and that natural convection effects are negligible in this region.

The maximum velocity U_{max} is an important quantity since it characterizes the effect of thermal buoyancy on the flow. Figure 5a shows the viscous boundary layer and the location of the local maximum velocity for $H/L = 0.68$, $Gr = 2.3 \times 10^6$, and $Re = 295$. The edge of the boundary layer is defined as the location where U/U_0 has a value of 0.99 for $U/U_0 < 1$ or 1.01 for $U/U_0 > 1$, respectively. This viscous boundary layer is seen to be much thicker than the thermal boundary layer in Fig. 3e. The peak in the velocity profiles shifts outward away from the surface and then merges with the forced flow far downstream. Fig. 5b shows the downstream variation of the local maximum velocity U_{max} for the same parameters as those in Fig. 5a. Also shown are some of the corresponding numerical results for negligible thickness.[14] It was found that a sharp change in the variation of the maximum velocity occurs in the vicinity of the top edge of the source because of the additional local input of thermal buoyancy, and these effects become negligible around $X = 3$. However, different trends are observed with significant module thickness. It is seen from this figure that local maximum velocity starts increasing gradually upstream near the heat source module due to the longitudinal conduction effects in the plate and the protruding effect of the module surface (A-B, see Fig. 1). It is also interesting to note the velocity maximum is found at $X = 1$, followed by a rapid decrease downstream in the vicinity of the module. This implies that the presence of the recirculation zone downstream of the module restricts the velocity development substantially to make the velocity maximum decrease to the forced flow value. Similar trends are found in numerical and experimental results of laminar flow over a backward-facing step.[20,21] However, only a qualitative comparison with these earlier studies can be made

because channel flows were considered in these instead of the extensive medium in the present study. It is again seen that the thermal buoyancy effects die out around $X = 3$, which is similar to that of Jaluria.[14]

The effect of the external flow on the surface temperature variation is shown at $H/L = 0.4$ and $Gr = 2.3 \times 10^6$ in Fig. 6. The heat source module is located from $X = 0$ to $X = 1$. It is seen that temperature starts rising gradually upstream of the source. This is a consequence of the longitudinal conduction transport in the plate and the protruding effect of the module surface A-B. The surface temperature rises sharply in the neighborhood of the heat source module. In the case of a heat source module located on a horizontal surface, the maximum temperature was observed at $X = 0.5$–1 depending on the Reynolds numbers.[16] However, for the vertical surface case studied here, the temperature maximum is always observed at $X = 1$ due to the natural convection effect near the top surface (C-D) of the heat source module. This maximum temperature is followed by a rapid drop. A more gradual temperature decay arises further downstream. The temperature level is found to be the highest for natural convection, compared to that for mixed or forced convection. This is an expected behavior since the combination of the buoyancy-driven flow and forced flow effects leads to a larger velocity level and consequent higher heat transfer coefficients. For a given heat input, a higher heat transfer rate results in lower temperatures. It is also seen that the temperature level decreases as the Reynolds number is increased.

Figure 7 shows the effect of the heat source module thickness on the surface temperature distribution for $Re = 295$ and $Gr = 2.3 \times 10^6$. Trends similar to those shown in Fig. 6 are observed. A substantial increase in the surface temperature downstream of the module is found with an increase in the module thickness H/L due to the recirculating flow at this zone. However, the thickness is found to have a small effect on the maximum temperature on the heat source module itself for the same Grashof number. Because of the nondimensionalization employed here, the Grashof number is based on the characteristic temperature difference, $q(L + 2H)k$. This indicates that the total energy input at the heat source module is the same for the same Grashof number even though the heat flux at the module surface decreases with an increase in the module thickness. For the same heat flux at the module surface, the Grashof number becomes larger with a thicker module. This implies, in turn, that the maximum surface temperature decreases with a decrease in the heat flux at the module surface for the same module thickness, as expected. This is a consequence of the fact that the total energy input at the heat source module decreases with a decrease in the heat flux at the module surface for the same module thickness.

The convective heat transfer coefficient can be presented in terms of the local Nusselt number Nu, which is defined as $Nu = hL/k$. Also, the local heat transfer coefficient h may be expressed in terms of the measured gradient at the module surface or of the measured surface heat flux, and the surface temperature. Thus,

$$Nu = \frac{hL}{k} = \frac{-\left.\frac{\partial T}{\partial x}\right|_w}{T_s - T_a} L = \frac{q_{\text{conv}} L}{(T_s - T_a)k}$$

(for the top and bottom surfaces of the module) (3)

$$Nu = \frac{-\left.\frac{\partial T}{\partial y}\right|_w}{T_s - T_a} L = \frac{q_{\text{conv}} L}{(T_s - T_a)k}$$

(for the side surface of the module) (4)

Here, the subscript w represents the relevant wall or surface. Also,

$$q_{\text{conv}} = q - q_{\text{cond}} \tag{5}$$

Here, q is the surface heat flux supplied by the electrical input. The heat flux conducted from the module to the test plate q_{cond} is measured by the heat flux gauges mounted on the backside of the heating strip in the module. The temperature gradients at the surface are obtained by using a second-order, least-squares curve fit to the measured temperature field. The values of the local Nusselt number obtained by these two methods were found to agree closely with each other. Even though the heat input into the fluid is highly localized, due to the heat source module, the idealized circumstance of a step change in the heat flux, with uniform heat flux over the source, clearly does not arise in the experiments.[7] The presence of a nonuniform heat flux affects the resulting local Nusselt number Nu.

The mean Nusselt number $\overline{Nu}$ for the module surface is defined as

$$\overline{Nu} = \frac{\overline{h}L}{k} \tag{6a}$$

where

$$\overline{Nu} = \frac{1}{A}\int_A Nu \, dA = \frac{1}{L + 2H}\int_{(L+2H)} h(s) \, ds \tag{6b}$$

Here, A is the total surface area of the module exposed to the fluid, i.e., $A = (L + 2H)\,W$, and s is the distance along the module surface, as shown in Fig. 8.

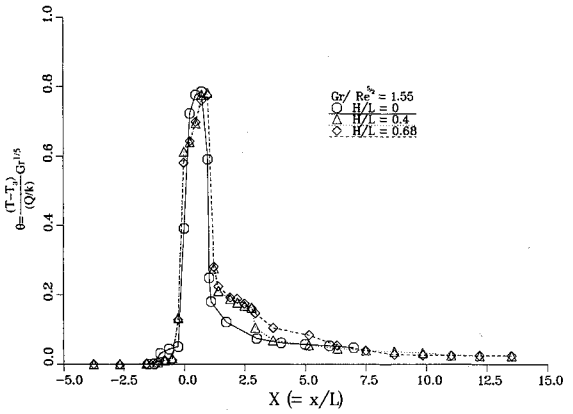

Fig. 7 Effect of the heat source module thickness on the surface-temperature variation at $Re = 295$ and $Gr = 2.3 \times 10^6$.

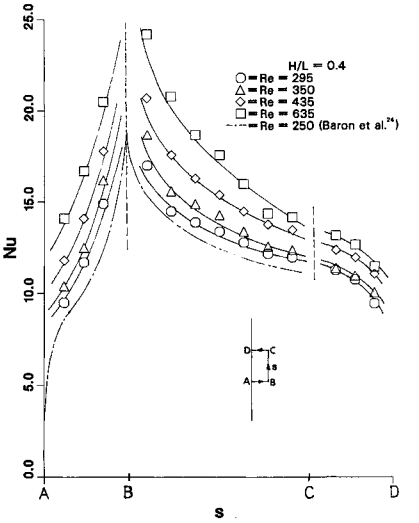

Fig. 8 The variation of the local Nusselt number Nu along the heat-source module surface at $H/L = 0.4$ and $Gr = 2.3 \times 10^6$.

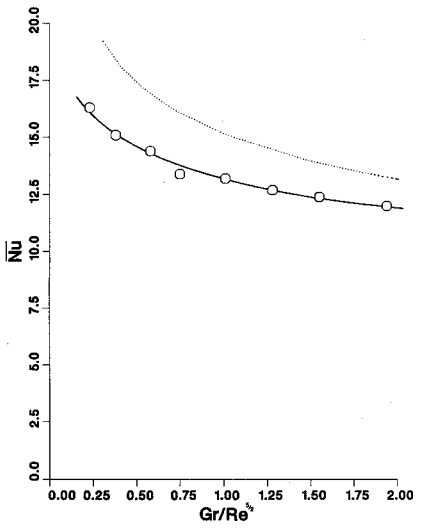

Fig. 9 The variation of the mean Nusselt number $\overline{Nu}$ with $Gr/Re^{5/2}$ for $Gr = 2.3 \times 10^6$:Θ $H/L = 0.4$, present study; ..., $H/L = 0$, analytical results.[26]

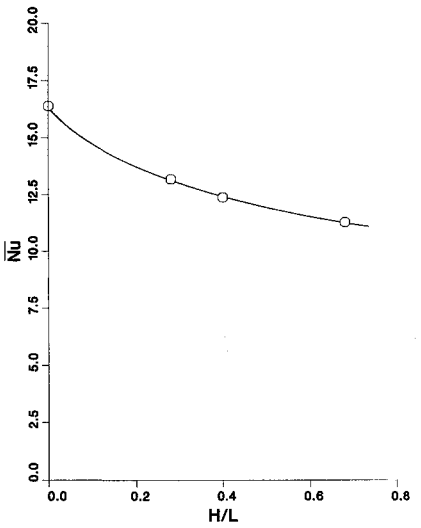

Fig. 10 The variation of the Mean Nusselt $\overline{Nu}$ with H/L for $Gr = 2.6 \times 10^6$ and $Re = 295$.

Employing the estimated uncertainty in each physical measurement, an uncertainty analysis for the experimental results is performed by the technique suggested by Moffat.[22,23] For instance, a simple determination of the relative uncertainty in the local Nusselt number $\delta Nu/Nu$ can be obtained using Eq. (3) or (4).

$$\frac{\delta Nu}{Nu} = \left[\left(\frac{\delta q_{conv}}{q_{conv}}\right)^2 + \left(\frac{\delta T_s}{T_s - T_a}\right)^2 + \left(\frac{\delta T_a}{T_s - T_a}\right)^2 + \left(\frac{\delta L}{L}\right)^2 + \left(\frac{\delta k}{k}\right)^2\right]^{1/2} \quad (7)$$

Since the error of the thermal conductivity k was estimated to be $\pm 2.5\%$ for the experimental conditions employed, the relative uncertainty in the local Nusselt number Nu was calculated to be 6% using Eq (7). Similarly, the relative uncertainties in Re and Gr were calculated to be 5 and 7%, respectively, using Eq. (2).

The variation of the local Nusselt number along the source surface is seen in Fig. 8 for $H/L = 0.4$ and $Gr = 2.3 \times 10^6$. The s coordinate employed for the local Nusselt number distribution includes both the vertical and the horizontal surfaces of the module. Also shown are the available numerical results associated with pure laminar flow over a forward-facing step and, thus, over only a portion of the source considered here.[24] However, the similarity between the present results and those of Baron and Tsou[24] is clearly seen, lending support to the results obtained here. The local Nusselt number Nu increases fairly uniformly along the front surface (A-B) of the module until the protruding corner (B) of the module. A maximum in Nu is observed near this corner at which the flow turns and the temperature contour lines are densely packed. Nu then decreases gradually, followed by a rapid decay over the module surface (C-D) due to the the recirculation flow. The trends obtained along the module surfaces (A-B) and (B-C) at this study show good agreement with those from the numerical calculations for a forward-facing step. The level of the numerical results are found to be lower than that of the experimental value because of the intensity of the forced convection flow effect. It is also seen, as expected, that Nu increases with an increase in the Reynolds number.

The mean Nusselt number $\overline{Nu}$ for $H/L = 0.4$ is plotted in Fig. 9 against the mixed convection parameter, $Gr/Re^{5/2}$, which represents the ratio of the buoyancy effects to the inertia effects. This parameter is obtained easily from a nondimensionalization of the governing equations and the boundary conditions for mixed convection flows with a uniform heat flux condition.[19,25] The mixed convection flow is termed natural convection dominated if the mixed convection parameter is significantly greater than unity. Similarly, if $Gr/Re^{5/2}$ is much smaller than unity, the flow is termed forced convection dominated. For a mixed convection parameter around unity, natural and forced convection effects are comparable in magnitude. In the present study, the mixed convection parameter was varied by changing the heat flux and/or the externally induced flow velocity to vary the mixed convection parameter over the range 0.2 to 2. As seen in Fig. 9, $\overline{Nu}$ decreases with an increase in the mixed convection parameter, but the effect of this parameter becomes smaller at larger values of $Gr/Re^{5/2}$. For a fixed Grashof number, the mixed convection parameter $Gr/Re^{5/2}$ decreases as the Reynolds number is increased. This indicates that the mean Nusselt number increases as the Reynolds number is increased. Also shown in this figure are the analytical results over the module with negligible thickness $H/L = 0$ for the forced convection case where the buoyancy effect by the heat source is assumed to be neglected.[26] The trends observed in the measurements are very similar to the analytical results. However, the quantative difference between the experimental and the analytical results is explained in terms of the effect of the module thickness.

The effect of the module thickness on $\overline{Nu}$ is shown in Fig. 10 at $Re = 295$ and $Gr = 2.3 \times 10^6$. It is found that $\overline{Nu}$ decreases as the module thickness H/L increases. As discussed in Fig. 8, the local heat transfer rate from the vertical surface (B-C) of the module is larger than that from the horizontal surfaces [(A-B) and (C-D)] of the module. When the module thickness H/L increases, the horizontal surfaces [(A-B) and (C-D)] also increase, and the vertical surface (B-C) is fixed as L. These increased horizontal surfaces result in the adverse effect of the mean Nusselt number. In addition, the heat flux becomes smaller with the increase of the module thickness for the same Grashof number because of nondimensionalization discussed earlier. This result indicates that the heat transport per unit area from a protruding heat module decreases as the thickness is increased for the same Grashof number when the module is mounted on a vertical surface.

Several other studies[27-29] have also considered such flows, particularly for the cooling of electronic equipment. However, the present study concerns mixed convection from protruding sources, which have received much less attention in the literature. The basic trends are, of course, in agreement with the earlier work. But the detailed aspects of the interaction between the wakes arising from the various surface elements of

the source and of the resulting thermal field have not been considered in the literature. Also we are interested in flows occurring in extensive media whereas much of the earlier work was related to channel flows. The flow is largely laminar over the parameter ranges considered. However, turbulence does arise far downstream, and a detailed investigation of the turbulent flow will be desirable from a practical viewpoint. The transition of the flow to turbulence is also an important consideration and needs further work.[19]

Conclusions

An experimental study of the mixed convective transport from a protruding heat source module mounted on a vertical, insulated plate has been carried out. The flow is obtained as two-dimensional and laminar with the experimental arrangement here. The effects of the mixed convection parameter and of the module thickness on the thermal fields, flowfields, and convective heat transfer rate were investigated in detail. The downstream behavior of the velocity and temperature fields is important in the positioning of other such heated elements, particularly in electronic circuitry and furnaces.

It is found that the isotherms become more densely packed around the module as the external flow increases and that the viscous boundary layer is much thicker than the thermal boundary layer for the same variables. It is also seen that the distortion of the flow around the module and the resulting temperature distribution in the flow are strongly affected by the module thickness. However, the module thickness has little influence on the maximum surface temperature on the module. This maximum temperature is always observed on the module top, horizontal surface (C-D). This is a consequence of the natural convection effect near the top surface (C-D) of the module. The surface temperature decreases with an increase in the Reynolds number, as expected.

The strong effect of the buoyancy force on the velocity profile is observed near the heat source module, and the recirculation zone appears at downstream locations near the top surface of the module because of the protruding effect. It is found that the protruding effects of the module and thermal buoyancy effects die out far downstream. The downstream variation of the local maximum velocity is strongly affected by the significant module thickness. It is also found that the thermal energy convected away from the heat source module decreases with an increase in the mixed convection parameter $Gr/Re^{5/2}$ and the module thickness, H/L for the same Grashof number.

Acknowledgments

The authors acknowledge the support of the National Science Foundation through Grant CBT-84-15364 for this work and the help of S. Tewari during the experimental work.

References

[1]Steinberg, D. S., *Cooling Techniques for Electronic Equipment,* Wiley, New York, 1980.

[2]Kraus, A. D., and Bar-Cohen, A., *Thermal Analysis Control of Electronic Equipment,* Hemisphere, New York, 1983.

Jaluria, Y., "Numerical Study of the Thermal Processes in a Furnace," *Numerical Heat Transfer,* Vol. 4, 1984, pp. 211-224.

[4]Gebhart, B., Jaluria, Y., Mahajan, R. L., and Sammakia, B., *Buoyancy-Induced Flows and Transports*, Hemisphere, New York, 1988.

[5]Jaluria, Y., and Gebhart, B., "Buoyancy-Induced Flow Arising from a Line Thermal Source on an Adiabatic Vertical Surface," *International Journal of Heat and Mass Transfer*, Vol. 20, 1977, pp. 153-157.

[6]Sparrow, E. M., Patankar, S. V., and Abdel-Washed, R. M., "Development of Wall and Free Plumes Above a Heated Vertical Plate," *Journal of Heat Transfer*, Vol. 100, 1978, pp. 184-190.

[7]Goel, S., and Jaluria, Y., "Thermal Transport from an Isolated Heated Source on the Vertical or Inclined Surface," *Proceedings of the 8th International Heat Transfer Conference*, Vol. 3, Hemisphere, New York, 1986, pp. 1341-1346.

[8]Carey, V. P., and Mollendorf, J. C., "The Temperature Field Above a Concentrated Heat Source on a Vertical Adiabatic Surface," *International Journal of Heat and Mass Transfer*, Vol. 20, 1977, pp. 1059-1067.

[9]Park, K.-A., and Bergles, A. E., "Natural Convection Heat Transfer Characteristics of Simulated Microelectronic Chips," *Journal of Heat Transfer*, Vol. 109, 1987, pp. 90-96.

[10]Afrid, M., and Zebib, A., "Natural Convection Cooling of Heated Components Mounted on a Vertical Wall," *Numerical Heat Transfer*, Vol. 15, 1989, pp. 243-259.

[11]Zebib, A., and Wo, Y. K., "A Two-Dimensional Conjugate Heat Transfer Model for Forced Air Cooling of an Electronic Device, *Journal of Electronic Packaging*, Vol. 111, 1989, pp. 41-45.

[12]Davaklath J., and Bayazitoglu, Y., "Forced Convection Cooling Across Rectangular Blocks, *Journal of Heat Transfer*, Vol. 109, 1987, pp. 321-328.

[13]Kennedy, K. J., and Zebib, A., "Combined Free and Forced Convection Between Horizontal Parallel Planes: Some Case Studies," *International Journal of Heat and Mass Transfer*, Vol. 26, 1983, pp. 471-474.

[14]Jaluria, Y., "Mixed Convection in a Wall Plume," *Computers and Fluids*, Vol. 10, 1982, pp. 95-105.

[15]Rao, K.V., Armaly, B.F., and Chen, T.S., "Analysis of Laminar Mixed Convection Plumes Along Vertical Adiabatic Surfaces," *Journal of Heat Transfer*, Vol. 106, 1984, pp. 552-557.

[16]Kang, B.H., Jaluria, Y., and Tewari, S., "Mixed Convection Air Cooling of an Isolated Rectangular Heat Source Module on a Horizontal Plate," *Proceedings of 25th National Heat Transfer Conference*, Vol. 2, ASME, New York, 1988, pp. 59-66.

[17]Tewari, S., and Jaluria, Y, "Natural and Mixed Convective Transport from Finite-Size Heat Sources on a Flat Plate in Cooling of Electronic Equipment," *The Thermofluid Mechanisms in Electronic Thermal Control Session of the Annual Winter Meeting of the ASME*, ASME, New York, 1987 pp. 1-9.

[18]Hollasch, K., and Gebhart, B., "Calibration of Constantan-Temperature Hot-Wire Anemometers at Low Velocities in Water with Variable Fluid Temperature," *Journal of Heat Transfer*, Vol. 94, 1972, pp. 17-22.

[19]Jaluria, Y., *Natural Convection Heat and Mass Transfer*, Pergamon Press, United Kingdom, 1980.

[20]Armaly, B. F., Durst, F., Pereira, J. C. F., and Schonung, B., "Experimental and Theoretical Investigation of Backward-Facing Step Flow," *Journal of Fluid Mechanics*, Vol. 127, 1983, pp. 473-496.

[21]Denham, M. K., and Patrick, M. A., "Laminar Flow over a Downstream-Facing Step in a Two-dimensional Flow Channel," *Transactions Institution of Chemical Engineers*, Vol. 52, 1974, pp. 361-367.

[22]Moffat, R. J., "Contributions to the Theory of Single-Sample Uncertainty Analysis," *Journal of Fluids Engineering*, Vol. 104, 1982, pp. 250-260.

[23]Moffat, R. J., "Using Uncertainty Analysis in the Planning of an Experiment," *Journal of Fluids Engineering*, Vol. 107, pp. 173-178.

[24]Baron, A., and Tsou, F.-K., "Flow Field and Heat Transfer Associated with Laminar Flow a Forward-Facing Step," *Proceedings of the 8th International Heat Transfer Conference*, Vol. 2, Hemisphere, New York, 1986, pp. 1077-1082.

[25]Jaluria, Y., Mixed Convection Flow Over Localized Multiple Thermal Sources on a Vertical Surface, *Physics of Fluids*, Vol. 29, 1986, pp. 934-940.

[26]Kays, W. M., and Crawford, M. E., *Convective Heat and Mass Transfer*, 2nd ed., McGraw-Hill, New York, 1980, p. 151.

[27]Churchill, S. W., "A Comprehensive Correlating Equation for Laminar, Assisting, Forced and Free Convection," *AIChE Journal*, Vol. 23, 1977, pp. 10 and 11.

[28]Heiber, C. A., "Laminar Mixed Convection in an Isothermal Horizontal Tube: Correlation of Heat Transfer Data," *International Journal of Heat and Mass Transfer*, Vol. 25, 1982, pp. 1737-1746.

[29]Aung, W., *Cooling Technology for Electronic Equipment*, Hemisphere, New York, 1988.